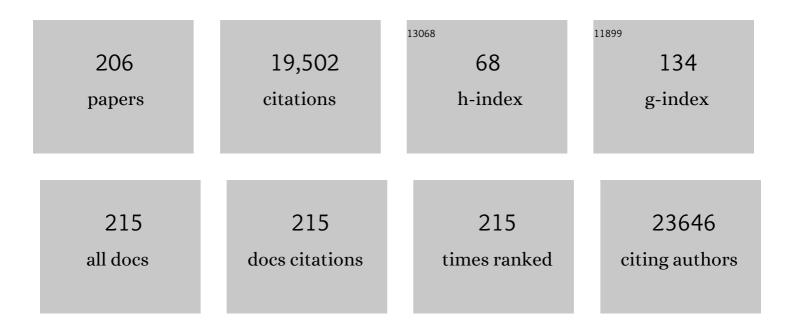
Bo Chen

List of Publications by Year in descending order

Source: https://exaly.com/author-pdf/834503/publications.pdf Version: 2024-02-01



RO CHEN

#	Article	IF	CITATIONS
1	2D Transitionâ€Metalâ€Dichalcogenideâ€Nanosheetâ€Based Composites for Photocatalytic and Electrocatalytic Hydrogen Evolution Reactions. Advanced Materials, 2016, 28, 1917-1933.	11.1	1,214
2	Two-Dimensional Metal Nanomaterials: Synthesis, Properties, and Applications. Chemical Reviews, 2018, 118, 6409-6455.	23.0	711
3	Iron-facilitated dynamic active-site generation on spinel CoAl2O4 with self-termination of surface reconstruction for water oxidation. Nature Catalysis, 2019, 2, 763-772.	16.1	678
4	Gut microbiota and intestinal FXR mediate the clinical benefits of metformin. Nature Medicine, 2018, 24, 1919-1929.	15.2	632
5	Carbon Fiber Aerogel Made from Raw Cotton: A Novel, Efficient and Recyclable Sorbent for Oils and Organic Solvents. Advanced Materials, 2013, 25, 5916-5921.	11.1	600
6	Synthesis of Two-Dimensional CoS _{1.097} /Nitrogen-Doped Carbon Nanocomposites Using Metal–Organic Framework Nanosheets as Precursors for Supercapacitor Application. Journal of the American Chemical Society, 2016, 138, 6924-6927.	6.6	591
7	Oneâ€pot Synthesis of CdS Nanocrystals Hybridized with Single‣ayer Transitionâ€Metal Dichalcogenide Nanosheets for Efficient Photocatalytic Hydrogen Evolution. Angewandte Chemie - International Edition, 2015, 54, 1210-1214.	7.2	584
8	Interdiffusion Reaction-Assisted Hybridization of Two-Dimensional Metal–Organic Frameworks and Ti ₃ C ₂ T _{<i>x</i>} Nanosheets for Electrocatalytic Oxygen Evolution. ACS Nano, 2017, 11, 5800-5807.	7.3	557
9	Bioinspired Design of Ultrathin 2D Bimetallic Metal–Organicâ€Framework Nanosheets Used as Biomimetic Enzymes. Advanced Materials, 2016, 28, 4149-4155.	11.1	440
10	Ultrathin Two-Dimensional Covalent Organic Framework Nanosheets: Preparation and Application in Highly Sensitive and Selective DNA Detection. Journal of the American Chemical Society, 2017, 139, 8698-8704.	6.6	440
11	Reduced Graphene Oxideâ€Wrapped MoO ₃ Composites Prepared by Using Metal–Organic Frameworks as Precursor for Allâ€Solidâ€State Flexible Supercapacitors. Advanced Materials, 2015, 27, 4695-4701.	11.1	388
12	Growth of Au Nanoparticles on 2D Metalloporphyrinic Metalâ€Organic Framework Nanosheets Used as Biomimetic Catalysts for Cascade Reactions. Advanced Materials, 2017, 29, 1700102.	11.1	384
13	Selfâ€Assembly of Single‣ayer CoAl‣ayered Double Hydroxide Nanosheets on 3D Graphene Network Used as Highly Efficient Electrocatalyst for Oxygen Evolution Reaction. Advanced Materials, 2016, 28, 7640-7645.	11.1	355
14	Enlarged CoO Covalency in Octahedral Sites Leading to Highly Efficient Spinel Oxides for Oxygen Evolution Reaction. Advanced Materials, 2018, 30, e1802912.	11.1	338
15	Oneâ€Pot Synthesis of Highly Anisotropic Fiveâ€Foldâ€Twinned PtCu Nanoframes Used as a Bifunctional Electrocatalyst for Oxygen Reduction and Methanol Oxidation. Advanced Materials, 2016, 28, 8712-8717.	11.1	336
16	Layered Transition Metal Dichalcogenideâ€Based Nanomaterials for Electrochemical Energy Storage. Advanced Materials, 2020, 32, e1903826.	11.1	329
17	Singleâ€Layer Transition Metal Dichalcogenide Nanosheetâ€Based Nanosensors for Rapid, Sensitive, and Multiplexed Detection of DNA. Advanced Materials, 2015, 27, 935-939.	11.1	322
18	MoS2 nanoflower-decorated reduced graphene oxide paper for high-performance hydrogen evolution reaction. Nanoscale, 2014, 6, 5624.	2.8	320

#	Article	IF	CITATIONS
19	Hybridization of MOFs and COFs: A New Strategy for Construction of MOF@COF Core–Shell Hybrid Materials. Advanced Materials, 2018, 30, 1705454.	11.1	318
20	Covalency competition dominates the water oxidation structure–activity relationship on spinel oxides. Nature Catalysis, 2020, 3, 554-563.	16.1	284
21	Controllable Design of MoS ₂ Nanosheets Anchored on Nitrogenâ€Doped Graphene: Toward Fast Sodium Storage by Tunable Pseudocapacitance. Advanced Materials, 2018, 30, e1800658.	11.1	275
22	Au Nanoparticleâ€Modified MoS ₂ Nanosheetâ€Based Photoelectrochemical Cells for Water Splitting. Small, 2014, 10, 3537-3543.	5.2	265
23	MOFâ€Based Hierarchical Structures for Solarâ€Thermal Clean Water Production. Advanced Materials, 2019, 31, e1808249.	11.1	233
24	Amorphous/Crystalline Heteroâ€Phase Pd Nanosheets: Oneâ€Pot Synthesis and Highly Selective Hydrogenation Reaction. Advanced Materials, 2018, 30, e1803234.	11.1	231
25	Synthesis of Ultrathin PdCu Alloy Nanosheets Used as a Highly Efficient Electrocatalyst for Formic Acid Oxidation. Advanced Materials, 2017, 29, 1700769.	11.1	207
26	Ultrathin Twoâ€Ðimensional Organic–Inorganic Hybrid Perovskite Nanosheets with Bright, Tunable Photoluminescence and High Stability. Angewandte Chemie - International Edition, 2017, 56, 4252-4255.	7.2	206
27	Silicate-Enhanced Heterogeneous Flow-Through Electro-Fenton System Using Iron Oxides under Nanoconfinement. Environmental Science & Technology, 2021, 55, 4045-4053.	4.6	192
28	Ethylene Selectivity in Electrocatalytic CO ₂ Reduction on Cu Nanomaterials: A Crystal Phase-Dependent Study. Journal of the American Chemical Society, 2020, 142, 12760-12766.	6.6	183
29	Tipâ€Enhanced Electric Field: A New Mechanism Promoting Mass Transfer in Oxygen Evolution Reactions. Advanced Materials, 2021, 33, e2007377.	11.1	179
30	Improved Reversibility of Fe ³⁺ /Fe ⁴⁺ Redox Couple in Sodium Super Ion Conductor Type Na ₃ Fe ₂ (PO ₄) ₃ for Sodiumâ€lon Batteries. Advanced Materials, 2017, 29, 1605694.	11.1	169
31	Coating Two-Dimensional Nanomaterials with Metal–Organic Frameworks. ACS Nano, 2014, 8, 8695-8701.	7.3	168
32	Carbonâ€Based Sorbents with Threeâ€Dimensional Architectures for Water Remediation. Small, 2015, 11, 3319-3336.	5.2	166
33	Ligandâ€Exchangeâ€Induced Amorphization of Pd Nanomaterials for Highly Efficient Electrocatalytic Hydrogen Evolution Reaction. Advanced Materials, 2020, 32, e1902964.	11.1	164
34	Crystal Phase and Architecture Engineering of Lotusâ€Thalamusâ€Shaped Ptâ€Ni Anisotropic Superstructures for Highly Efficient Electrochemical Hydrogen Evolution. Advanced Materials, 2018, 30, e1801741.	11.1	163
35	Molten Salt-Directed Catalytic Synthesis of 2D Layered Transition-Metal Nitrides for Efficient Hydrogen Evolution. CheM, 2020, 6, 2382-2394.	5.8	163
36	Flood-induced mortality across the globe: Spatiotemporal pattern and influencing factors. Science of the Total Environment, 2018, 643, 171-182.	3.9	156

ą	#	Article	IF	CITATIONS
;	37	Surfactant assisted Ce–Fe mixed oxide decorated multiwalled carbon nanotubes and their arsenic adsorption performance. Journal of Materials Chemistry A, 2013, 1, 11355.	5.2	151
;	38	Metal–organic framework-derived mesoporous carbon nanoframes embedded with atomically dispersed Fe–N active sites for efficient bifunctional oxygen and carbon dioxide electroreduction. Applied Catalysis B: Environmental, 2020, 267, 118720.	10.8	151
;	39	Submonolayered Ru Deposited on Ultrathin Pd Nanosheets used for Enhanced Catalytic Applications. Advanced Materials, 2016, 28, 10282-10286.	11.1	148
4	40	Synthesis of PdM (M = Zn, Cd, ZnCd) Nanosheets with an Unconventional Face-Centered Tetragonal Phase as Highly Efficient Electrocatalysts for Ethanol Oxidation. ACS Nano, 2019, 13, 14329-14336.	7.3	133
4	41	Preparation of Single‣ayer MoS ₂ <i>_x</i> Se _{2(1â€} <i>_x</i> Se _{2(1â€} <i>_x</i> Se _x Mo <i>_x</i> Se _x	5.2	126
4	42	Hydrogen-Intercalation-Induced Lattice Expansion of Pd@Pt Core–Shell Nanoparticles for Highly Efficient Electrocatalytic Alcohol Oxidation. Journal of the American Chemical Society, 2021, 143, 11262-11270.	6.6	121
4	43	Metastable 1T′-phase group VIB transition metal dichalcogenide crystals. Nature Materials, 2021, 20, 1113-1120.	13.3	119
4	44	Synthesis of RuNi alloy nanostructures composed of multilayered nanosheets for highly efficient electrocatalytic hydrogen evolution. Nano Energy, 2019, 66, 104173.	8.2	116
4	45	MoS2-coated vertical graphene nanosheet for high-performance rechargeable lithium-ion batteries and hydrogen production. NPG Asia Materials, 2016, 8, e268-e268.	3.8	113
4	46	Phase-Selective Epitaxial Growth of Heterophase Nanostructures on Unconventional 2H-Pd Nanoparticles. Journal of the American Chemical Society, 2020, 142, 18971-18980.	6.6	111
4	47	DNAâ€Templated Silver Nanoclusters for Multiplexed Fluorescent DNA Detection. Small, 2015, 11, 1385-1389.	5.2	106
2	48	Intercalation of organics into layered structures enables superior interface compatibility and fast charge diffusion for dendrite-free Zn anodes. Energy and Environmental Science, 2022, 15, 1682-1693.	15.6	105
	49	Preparation of 1T′-Phase ReS _{2<i>x</i>} Se _{2(1-<i>x</i>)} (<i>x</i> = 0–1) Nanodots for Highly Efficient Electrocatalytic Hydrogen Evolution Reaction. Journal of the American Chemical Society, 2018, 140, 8563-8568.	6.6	104
4	50	In Situ Synthesis of Metal Sulfide Nanoparticles Based on 2D Metalâ€Organic Framework Nanosheets. Small, 2016, 12, 4669-4674.	5.2	101
:	51	Selective Epitaxial Growth of Oriented Hierarchical Metal–Organic Framework Heterostructures. Journal of the American Chemical Society, 2020, 142, 8953-8961.	6.6	100
4	52	Synthesis of Palladiumâ€Based Crystalline@Amorphous Core–Shell Nanoplates for Highly Efficient Ethanol Oxidation. Advanced Materials, 2020, 32, e2000482.	11.1	98
;	53	Bifunctional single-molecular heterojunction enables completely selective CO ₂ -to-CO conversion integrated with oxidative 3D nano-polymerization. Energy and Environmental Science, 2021, 14, 1544-1552.	15.6	95
-	54	Transmembrane Delivery of the Cell-Penetrating Peptide Conjugated Semiconductor Quantum Dots. Langmuir, 2008, 24, 11866-11871.	1.6	92

#	Article	IF	CITATIONS
55	Heterophase fcc-2H-fcc gold nanorods. Nature Communications, 2020, 11, 3293.	5.8	92
56	Liquidâ€Phase Epitaxial Growth of Twoâ€Dimensional Semiconductor Heteroâ€nanostructures. Angewandte Chemie - International Edition, 2015, 54, 1841-1845.	7.2	88
57	Preparation of Au@Pd Core–Shell Nanorods with <i>fcc</i> -2H- <i>fcc</i> Heterophase for Highly Efficient Electrocatalytic Alcohol Oxidation. Journal of the American Chemical Society, 2022, 144, 547-555.	6.6	88
58	Intramolecular Hydrogen Bonding-Based Topology Regulation of Two-Dimensional Covalent Organic Frameworks. Journal of the American Chemical Society, 2020, 142, 13162-13169.	6.6	85
59	Progressively Exposing Active Facets of 2D Nanosheets toward Enhanced Pseudocapacitive Response and Highâ€Rate Sodium Storage. Advanced Materials, 2019, 31, e1900526.	11.1	83
60	Confined Growth of Silver–Copper Janus Nanostructures with {100} Facets for Highly Selective Tandem Electrocatalytic Carbon Dioxide Reduction. Advanced Materials, 2022, 34, e2110607.	11.1	82
61	Quantification of Cancer Biomarkers in Serum Using Scattering-Based Quantitative Single Particle Intensity Measurement with a Dark-Field Microscope. Analytical Chemistry, 2016, 88, 8849-8856.	3.2	81
62	Synthesis of Hierarchical 4H/fcc Ru Nanotubes for Highly Efficient Hydrogen Evolution in Alkaline Media. Small, 2018, 14, e1801090.	5.2	80
63	Size-Controlled and Size-Designed Synthesis of Nano/Submicrometer Ag Particles. Crystal Growth and Design, 2010, 10, 3378-3386.	1.4	79
64	Geology and geochemistry of the Baijiantan–Baikouquan ophiolitic mélanges: implications for geological evolution of west Junggar, Xinjiang, NW China. Geological Magazine, 2015, 152, 41-69.	0.9	78
65	A bright carbon-dot-based fluorescent probe for selective and sensitive detection of mercury ions. Talanta, 2016, 161, 476-481.	2.9	75
66	Aging amorphous/crystalline heterophase PdCu nanosheets for catalytic reactions. National Science Review, 2019, 6, 955-961.	4.6	75
67	Heterostructured TiO ₂ Spheres with Tunable Interiors and Shells toward Improved Packing Density and Pseudocapacitive Sodium Storage. Advanced Materials, 2019, 31, e1904589.	11.1	73
68	Characteristics of aquatic bacterial community and the influencing factors in an urban river. Science of the Total Environment, 2016, 569-570, 382-389.	3.9	72
69	AuAg Nanosheets Assembled from Ultrathin AuAg Nanowires. Journal of the American Chemical Society, 2015, 137, 1444-1447.	6.6	68
70	Ultrathin Amorphous/Crystalline Heterophase Rh and Rh Alloy Nanosheets as Tandem Catalysts for Direct Indole Synthesis. Advanced Materials, 2021, 33, e2006711.	11.1	68
71	Transformable masks for colloidal nanosynthesis. Nature Communications, 2018, 9, 563.	5.8	67
72	Synthesis of Pd ₃ Sn and PdCuSn Nanorods with <i>L1₂</i> Phase for Highly Efficient Electrocatalytic Ethanol Oxidation. Advanced Materials, 2022, 34, e2106115.	11.1	65

#	Article	IF	CITATIONS
73	Evoking ordered vacancies in metallic nanostructures toward a vacated Barlow packing for high-performance hydrogen evolution. Science Advances, 2021, 7, .	4.7	64
74	Electronic Effect Directed Au(I)-Catalyzed Cyclic C2–H Bond Functionalization of 3-Allenylindoles. Organic Letters, 2012, 14, 3616-3619.	2.4	63
75	Composition- and phase-controlled synthesis and applications of alloyed phase heterostructures of transition metal disulphides. Nanoscale, 2017, 9, 5102-5109.	2.8	63
76	Preparation of Ultrathin Twoâ€Dimensional Ti _{<i>x</i>} Ta _{1â^'<i>x</i>} S _{<i>y</i>} O _{<i>z</i>} Nanosheets as Highly Efficient Photothermal Agents. Angewandte Chemie - International Edition, 2017, 56, 7842-7846.	7.2	59
77	Seeded Synthesis of Unconventional 2H-Phase Pd Alloy Nanomaterials for Highly Efficient Oxygen Reduction. Journal of the American Chemical Society, 2021, 143, 17292-17299.	6.6	59
78	Anodized Aluminum Oxide Templated Synthesis of Metal–Organic Frameworks Used as Membrane Reactors. Angewandte Chemie - International Edition, 2017, 56, 578-581.	7.2	57
79	Selective Epitaxial Growth of Rh Nanorods on 2H/ <i>fcc</i> Heterophase Au Nanosheets to Form 1D/2D Rh–Au Heterostructures for Highly Efficient Hydrogen Evolution. Journal of the American Chemical Society, 2021, 143, 4387-4396.	6.6	56
80	N- and S- co-doped graphene sheet-encapsulated Co9S8 nanomaterials as excellent electrocatalysts for the oxygen evolution reaction. Journal of Power Sources, 2019, 417, 90-98.	4.0	52
81	Single-crystalline Bi ₂ Fe ₄ O ₉ synthesized by low-temperature co-precipitation: performance as photo- and Fenton catalysts. RSC Advances, 2014, 4, 27820-27829.	1.7	51
82	Suppressing the intestinal farnesoid X receptor/sphingomyelin phosphodiesterase 3 axis decreases atherosclerosis. Journal of Clinical Investigation, 2021, 131, .	3.9	50
83	Chitosan nanoparticles for loading of toothpaste actives and adhesion on tooth analogs. Journal of Applied Polymer Science, 2007, 106, 4248-4256.	1.3	49
84	Realization of vertical metal semiconductor heterostructures via solution phase epitaxy. Nature Communications, 2018, 9, 3611.	5.8	49
85	Preparation of <i>fcc</i> â€2Hâ€ <i>fcc</i> Heterophase Pd@Ir Nanostructures for Highâ€Performance Electrochemical Hydrogen Evolution. Advanced Materials, 2022, 34, e2107399.	11.1	48
86	Weavable, Highâ€Performance, Solidâ€State Supercapacitors Based on Hybrid Fibers Made of Sandwiched Structure of MWCNT/rGO/MWCNT. Advanced Electronic Materials, 2016, 2, 1600102.	2.6	47
87	Self-Assembled Fluorescent Bovine Serum Albumin Nanoprobes for Ratiometric pH Measurement inside Living Cells. ACS Applied Materials & Interfaces, 2016, 8, 9629-9634.	4.0	47
88	Optical Spectroscopy of Single Colloidal CsPbBr ₃ Perovskite Nanoplatelets. Nano Letters, 2020, 20, 3673-3680.	4.5	47
89	Elemental Segregation in Multimetallic Core–Shell Nanoplates. Journal of the American Chemical Society, 2019, 141, 14496-14500.	6.6	46
90	Ruthenium nanoclusters anchored on cobalt phosphide hollow microspheres by green phosphating process for full water splitting in acidic electrolyte. Chinese Chemical Letters, 2021, 32, 511-515.	4.8	46

#	Article	IF	CITATIONS
91	Transforming Monolayer Transition-Metal Dichalcogenide Nanosheets into One-Dimensional Nanoscrolls with High Photosensitivity. ACS Applied Materials & Interfaces, 2018, 10, 13011-13018.	4.0	45
92	Synthesis of MoX2 (X = Se or S) monolayers with high-concentration 1T′ phase on 4H/fcc-Au nanorods for hydrogen evolution. Nano Research, 2019, 12, 1301-1305.	5.8	44
93	A Gasâ€Phase Migration Strategy to Synthesize Atomically Dispersed Mnâ€Nâ€C Catalysts for Zn–Air Batteries. Small Methods, 2021, 5, e2100024.	4.6	44
94	Effect of glutenin and gliadin modified by protein-glutaminase on retrogradation properties and digestibility of potato starch. Food Chemistry, 2019, 301, 125226.	4.2	43
95	Hybrid Flexible Resistive Random Access Memoryâ€Gated Transistor for Novel Nonvolatile Data Storage. Small, 2016, 12, 390-396.	5.2	42
96	Isoreticular Series of Two-Dimensional Covalent Organic Frameworks with the kgd Topology and Controllable Micropores. Journal of the American Chemical Society, 2022, 144, 6475-6482.	6.6	41
97	Highly stable magnetic multiwalled carbon nanotube composites for solid-phase extraction of linear alkylbenzene sulfonates in environmental water samples prior to high-performance liquid chromatography analysis. Analyst, The, 2012, 137, 1232.	1.7	39
98	Decreasing the Overpotential of Aprotic Li O ₂ Batteries with the Inâ€Plane Alloy Structure in Ultrathin 2D Ruâ€Based Nanosheets. Advanced Functional Materials, 2022, 32, .	7.8	39
99	A fluorometric biosensor based on H2O2-sensitive nanoclusters for the detection of acetylcholine. Biosensors and Bioelectronics, 2014, 59, 289-292.	5.3	38
100	Rapid Analysis of Bisphenol A and Its Analogues in Food Packaging Products by Paper Spray Ionization Mass Spectrometry. Journal of Agricultural and Food Chemistry, 2017, 65, 4859-4865.	2.4	38
101	In vitro evaluation of cytotoxicity and oxidative stress induced by multiwalled carbon nanotubes in murine RAW 264.7 macrophages and human A549 lung cells. Biomedical and Environmental Sciences, 2011, 24, 593-601.	0.2	38
102	Fabrication of folic acid-sensitive gold nanoclusters for turn-on fluorescent imaging of overexpression of folate receptor in tumor cells. Talanta, 2016, 158, 118-124.	2.9	36
103	NaF-mediated controlled-synthesis of multicolor Na _x ScF _{3+x} :Yb/Er upconversion nanocrystals. Nanoscale, 2015, 7, 4048-4054.	2.8	33
104	A universal method for rapid and largeâ€scale growth of layered crystals. SmartMat, 2020, 1, e1011.	6.4	33
105	Crystal phase-controlled growth of PtCu and PtCo alloys on 4H Au nanoribbons for electrocatalytic ethanol oxidation reaction. Nano Research, 2020, 13, 1970-1975.	5.8	32
106	Bioinspired Synthesis of Nortriterpenoid Propindilactone G. Journal of the American Chemical Society, 2020, 142, 5007-5012.	6.6	32
107	Macrophage HIF-2α suppresses NLRP3 inflammasome activation and alleviates insulin resistance. Cell Reports, 2021, 36, 109607.	2.9	32
108	New urea-modified paper substrate for enhanced analytical performance of negative ion mode paper spray mass spectrometry. Talanta, 2017, 166, 306-314.	2.9	31

#	Article	IF	CITATIONS
109	Free-standing 2D nanorafts by assembly of 1D nanorods for biomolecule sensing. Nanoscale, 2019, 11, 12169-12176.	2.8	30
110	Rapid analysis of benzoic acid and vitamin C in beverages by paper spray mass spectrometry. Food Chemistry, 2018, 268, 411-415.	4.2	29
111	Glutathione-mediated formation of disulfide bonds modulates the properties of myofibrillar protein gels at different temperatures. Food Chemistry, 2021, 364, 130356.	4.2	29
112	Preparation of Amorphous SnO ₂ â€Encapsulated Multiphased Crystalline Cu Heterostructures for Highly Efficient CO ₂ Reduction. Advanced Materials, 2022, 34, e2201114.	11.1	29
113	Two-dimensional molybdenum disulphide nanosheet-covered metal nanoparticle array as a floating gate in multi-functional flash memories. Nanoscale, 2015, 7, 17496-17503.	2.8	28
114	Transition metal dichalcogenide/multi-walled carbon nanotube-based fibers as flexible electrodes for electrocatalytic hydrogen evolution. Chemical Communications, 2020, 56, 5131-5134.	2.2	28
115	Preparation of graphene-MoS2 hybrid aerogels as multifunctional sorbents for water remediation. Science China Materials, 2017, 60, 1102-1108.	3.5	27
116	An assessment of melamine exposure in Shanghai adults and its association with food consumption. Environment International, 2020, 135, 105363.	4.8	27
117	Defect-Rich Hierarchical Porous UiO-66(Zr) for Tunable Phosphate Removal. Environmental Science & Technology, 2021, 55, 13209-13218.	4.6	27
118	Hybridization of 2D Nanomaterials with 3D Graphene Architectures for Electrochemical Energy Storage and Conversion. Advanced Functional Materials, 2022, 32, .	7.8	26
119	Unusual 4H-phase twinned noble metal nanokites. Nature Communications, 2019, 10, 2881.	5.8	25
120	Additive-assisted synthesis of boride, carbide, and nitride micro/nanocrystals. Journal of Solid State Chemistry, 2012, 194, 219-224.	1.4	24
121	General Fabrication of Boride, Carbide, and Nitride Nanocrystals via a Metal-Hydrolysis-Assisted Process. Inorganic Chemistry, 2017, 56, 2440-2447.	1.9	23
122	Water transport confined in graphene oxide channels through the rarefied effect. Physical Chemistry Chemical Physics, 2018, 20, 9780-9786.	1.3	23
123	Rapid Analysis of Illegal Cationic Dyes in Foods and Surface Waters Using High Temperature Direct Analysis in Real Time High-Resolution Mass Spectrometry. Journal of Agricultural and Food Chemistry, 2018, 66, 7542-7549.	2.4	23
124	Defect-Rich, Candied Haws-Shaped AuPtNi Alloy Nanostructures for Highly Efficient Electrocatalysis. CCS Chemistry, 2020, 2, 24-30.	4.6	23
125	Precise Dimerization of Hollow Fullerene Compartments. Journal of the American Chemical Society, 2020, 142, 15396-15402.	6.6	22
126	Impeding Catalyst Sulfur Poisoning in Aqueous Solution by Metal–Organic Framework Composites. Small Methods, 2020, 4, 1900890.	4.6	22

#	Article	IF	CITATIONS
127	Single Particle Tracking of Peptides-Modified Nanocargo on Lipid Membrane Revealing Bulk-Mediated Diffusion. Analytical Chemistry, 2016, 88, 11973-11977.	3.2	21
128	Facile "one-pot―synthesis of poly(methacrylic acid)-based hybrid monolith via thiol-ene click reaction for hydrophilic interaction chromatography. Journal of Chromatography A, 2016, 1454, 49-57.	1.8	21
129	Synthesis of WO _{<i>n</i>} â€WX ₂ (<i>n</i> =2.7, 2.9; X=S, Se) Heterostructures for Highly Efficient Green Quantum Dot Lightâ€Emitting Diodes. Angewandte Chemie - International Edition, 2017, 56, 10486-10490.	7.2	21
130	Spatial Variability and Temporal Persistence of Event Runoff Coefficients for Cropland Hillslopes. Water Resources Research, 2019, 55, 1583-1597.	1.7	21
131	Pulsed elution modulation for on-line comprehensive two-dimensional liquid chromatography coupling reversed phase liquid chromatography and hydrophilic interaction chromatography. Journal of Chromatography A, 2019, 1583, 98-107.	1.8	21
132	Construction of a Sandwiched MOF@COF Composite as a Size-Selective Catalyst. Cell Reports Physical Science, 2020, 1, 100272.	2.8	21
133	Phosphineâ€Free, Lowâ€Temperature Synthesis of Tetrapodâ€Shaped CdS and Its Hybrid with Au Nanoparticles. Small, 2014, 10, 4727-4734.	5.2	20
134	An iTRAQ-Based Proteomics Approach to Clarify the Molecular Physiology of Somatic Embryo Development in Prince Rupprecht's Larch (Larix principis-rupprechtii Mayr). PLoS ONE, 2015, 10, e0119987.	1.1	20
135	Synthesis of high-quality lanthanide oxybromides nanocrystals with single-source precursor for promising applications in cancer cells imaging. Applied Materials Today, 2015, 1, 20-26.	2.3	20
136	Association of Dietary Pattern during Pregnancy and Gestational Diabetes Mellitus: A Prospective Cohort Study in Northern China. Biomedical and Environmental Sciences, 2017, 30, 887-897.	0.2	19
137	Saltâ€Assisted 2Hâ€ŧoâ€1T′ Phase Transformation of Transition Metal Dichalcogenides. Advanced Materials, 2022, 34, e2201194.	11.1	19
138	Controlled Synthesis of Uniform Na _{<i>x</i>} ScF _{3+<i>x</i>} Nanopolyhedrons, Nanoplates, Nanorods, and Nanospheres Using Solvents. Crystal Growth and Design, 2015, 15, 2988-2993.	1.4	18
139	Rapid analysis of Aurantii Fructus Immaturus (Zhishi) using paper spray ionization mass spectrometry. Journal of Pharmaceutical and Biomedical Analysis, 2017, 137, 204-212.	1.4	18
140	Anodized Aluminum Oxide Templated Synthesis of Metal–Organic Frameworks Used as Membrane Reactors. Angewandte Chemie, 2017, 129, 593-596.	1.6	18
141	Stochastic micromechanical predictions for the probabilistic behavior of saturated concrete repaired by the electrochemical deposition method. International Journal of Damage Mechanics, 2020, 29, 435-453.	2.4	18
142	Liquid Nanoparticles: Manipulating the Nucleation and Growth of Nanoscale Droplets. Angewandte Chemie - International Edition, 2021, 60, 3047-3054.	7.2	18
143	Quasiâ€Epitaxial Growth of Magnetic Nanostructures on 4Hâ€Au Nanoribbons. Advanced Materials, 2021, 33, e2007140.	11.1	18
144	Intensive Versus Extensive Events? Insights from Cumulative Flood-Induced Mortality Over the Globe, 1976–2016. International Journal of Disaster Risk Science, 2020, 11, 441-451.	1.3	17

#	Article	IF	CITATIONS
145	The establishment of the fertile fish lineages derived from distant hybridization by overcoming the reproductive barriers. Reproduction, 2020, 159, R237-R249.	1.1	17
146	Two-dimensional covalent organic framework nanosheets: Synthesis and energy-related applications. Chinese Chemical Letters, 2022, 33, 2867-2882.	4.8	17
147	TaS2 nanosheet-based room-temperature dosage meter for nitric oxide. APL Materials, 2014, 2, .	2.2	16
148	Facile synthesis of Cu ₂ O nanocages and gas sensing performance towards gasoline. RSC Advances, 2015, 5, 54433-54438.	1.7	16
149	A simple electrochemical method for conversion of Pt wires to Pt concave icosahedra and nanocubes on carbon paper for electrocatalytic hydrogen evolution. Science China Materials, 2019, 62, 115-121.	3.5	16
150	Sizeâ€Dependent Phase Transformation of Noble Metal Nanomaterials. Small, 2019, 15, e1903253.	5.2	16
151	Rapid analysis of Callicarpa L. using direct spray ionization mass spectrometry. Journal of Pharmaceutical and Biomedical Analysis, 2016, 124, 93-103.	1.4	15
152	Imparting Boron Nanosheets with Ambient Stability through Methyl Group Functionalization for Mechanistic Investigation of Their Lithiation Process. ACS Applied Materials & Interfaces, 2020, 12, 23370-23377.	4.0	15
153	Bimetallic Bi–Sn microspheres as high initial coulombic efficiency and long lifespan anodes for sodium-ion batteries. Chemical Communications, 2022, 58, 5140-5143.	2.2	15
154	Rapid Analysis of <i>Corni fructus</i> Using Paper Sprayâ€Mass Spectrometry. Phytochemical Analysis, 2017, 28, 344-350.	1.2	14
155	Bimetallic oxide coupled with B-doped graphene as highly efficient electrocatalyst for oxygen evolution reaction. Science China Materials, 2020, 63, 1247-1256.	3.5	14
156	The preparation of a poly (pentaerythritol tetraglycidyl ether-co-poly ethylene imine) organic monolithic capillary column and its application in hydrophilic interaction chromatography for polar molecules. Analytica Chimica Acta, 2017, 988, 104-113.	2.6	12
157	Rapid quantitative analysis of ginkgo flavonoids using paper spray mass spectrometry. Journal of Pharmaceutical and Biomedical Analysis, 2019, 171, 158-163.	1.4	12
158	Levelling the playing field: screening for synergistic effects in coalesced bimetallic nanoparticles. Nanoscale, 2016, 8, 3447-3453.	2.8	11
159	Quantifying the Distribution of the Stoichiometric Composition of Anticancer Peptide Lycosin-I on the Lipid Membrane with Single Molecule Spectroscopy. Journal of Physical Chemistry B, 2016, 120, 3081-3088.	1.2	11
160	Preparation of Ultrathin Twoâ€Đimensional Ti _{<i>x</i>} Ta _{1â^'<i>x</i>} S _{<i>y</i>} O _{<i>z</i>} Nanosheets as Highly Efficient Photothermal Agents. Angewandte Chemie, 2017, 129, 7950-7954.	1.6	11
161	Preparation of CdS <i>_y</i> Se _{1â^<} <i>_y</i> â€MoS ₂ Heterostructures via Cation Exchange of Preâ€Epitaxially Synthesized Cu _{2â^} <i>_{ï‡}</i> Si> _y Se _{1â^<} <i>_y</i> for Photocatalytic Hydrogen Evolution, Small, 2021, 17, e2006135.	sub ² 2 <td>ıb¹¹</td>	ıb ¹¹
162	Structure of the Upper Mantle and Transition Zone Beneath the South China Block Imaged by Finite Frequency Tomography. Acta Geologica Sinica, 2016, 90, 1637-1652.	0.8	10

#	Article	IF	CITATIONS
163	Facile fabrication of hydrophobic octadecylamine-functionalized polyurethane foam for oil spill cleanup. Journal of Macromolecular Science - Pure and Applied Chemistry, 2016, 53, 196-200.	1.2	9
164	The synthesis of Gemini-type sulfobetaine based hybrid monolith and its application in hydrophilic interaction chromatography for small polar molecular. Talanta, 2017, 173, 113-122.	2.9	9
165	Construction of 4â€Isochromanones through Cu(OTf) ₂ â€Catalysed Sequential C=O and C–O Bond Formation. European Journal of Organic Chemistry, 2018, 2018, 926-931.	1.2	9
166	Preparation of fine-grained α-alumina powder from seeded boehmite. Journal of Nanoparticle Research, 2013, 15, 1.	0.8	8
167	Orthogonal strategy development using reversed macroporous resin coupled with hydrophilic interaction liquid chromatography for the separation of ginsenosides from ginseng root extract. Journal of Separation Science, 2017, 40, 4128-4134.	1.3	8
168	Natural meroterpenoids isolated from the plant pathogenic fungus Verticillium albo-atrum with noteworthy modification action against voltage-gated sodium channels of central neurons of Helicoverpa armigera. Pesticide Biochemistry and Physiology, 2018, 144, 91-99.	1.6	8
169	Synthesis of a poly(sulfobetaine-co-polyhedral oligomeric silsesquioxane) hybrid monolith via an in-situ ring opening quaternization for use in hydrophilic interaction capillary liquid chromatography. Mikrochimica Acta, 2020, 187, 109.	2.5	8
170	High‥ield Exfoliation of Ultrathin 2D Ni ₃ Cr ₂ P ₂ S ₉ and Ni ₃ Cr ₂ P ₂ Se ₉ Nanosheets. Small, 2021, 17, e2006866.	5.2	8
171	Microfluidic Chip-Based Induced Phase Separation Extraction as a Fast and Efficient Miniaturized Sample Preparation Method. Molecules, 2021, 26, 38.	1.7	8
172	Fabrication of hollow cubic Ag microboxes with net-like nanofiber structures and their surface plasmon resonance. CrystEngComm, 2011, 13, 204-211.	1.3	7
173	The synthesis of surface-glycosylated porous monolithic column via aqueous two-phase graft copolymerization and its application in capillary-liquid chromatography. Talanta, 2016, 161, 721-729.	2.9	7
174	Synthesis of WO _{<i>n</i>} â€WX ₂ (<i>n</i> =2.7, 2.9; X=S, Se) Heterostructures for Highly Efficient Green Quantum Dot Lightâ€Emitting Diodes. Angewandte Chemie, 2017, 129, 10622-10626.	1.6	7
175	The fabrication of poly (polyethylene glycol diacrylate) monolithic porous layer open tubular (monoâ&PLOT) columns and applications in hydrophilic interaction chromatography and capillary gas chromatography for small molecules. Electrophoresis, 2019, 40, 521-529.	1.3	7
176	Development of Biomimetic Synthesis of Propindilactone G ^{â€} . Chinese Journal of Chemistry, 2020, 38, 1339-1352.	2.6	7
177	Mesocarbon Microbeads Boost the Electrochemical Performances of LiFePO ₄ Li ₄ Ti ₅ O ₁₂ through Anion Intercalation. ChemSusChem, 2022, 15, .	3.6	7
178	Polymerization of polyhedral oligomeric silsequioxane (POSS) with perfluoro-monomers and a kinetic study. RSC Advances, 2017, 7, 10700-10706.	1.7	5
179	The colour combination method for human-machine interfaces driven by colour images. Journal of Engineering Design, 2017, 28, 505-531.	1.1	5
180	Analysis of Chromosomal Numbers, Mitochondrial Genome, and Full-Length Transcriptome of Onychostoma brevibarba. Marine Biotechnology, 2019, 21, 515-525.	1.1	5

#	Article	IF	CITATIONS
181	Research on the Dynamic Path Planning of Manipulators Based on a Grid-Local Probability Road Map Method. IEEE Access, 2021, 9, 101186-101196.	2.6	5
182	Land Subsidence in Qingdao, China, from 2017 to 2020 Based on PS-InSAR. International Journal of Environmental Research and Public Health, 2022, 19, 4913.	1.2	5
183	Application of 1-Alkyl-3-methylimidazolium-Based Ionic Liquids as Background Electrolytes in Nonaqueous Capillary Electrophoresis for the Analysis of Coptidis Alkaloids. Analytical Letters, 2012, 45, 460-472.	1.0	4
184	Characterization of Oxygenates in Zhundong Subbituminous Coal by Gas Chromatography/Mass Spectrometry. Analytical Letters, 2016, 49, 1359-1365.	1.0	4
185	Rapid analysis of benzalkonium chloride using paper spray mass spectrometry. Journal of Pharmaceutical and Biomedical Analysis, 2017, 145, 151-157.	1.4	4
186	A River Channel Extraction Method for Urban Environments Based on Terrain Transition Lines. Water Resources Research, 2018, 54, 4887-4900.	1.7	4
187	Liquid Nanoparticles: Manipulating the Nucleation and Growth of Nanoscale Droplets. Angewandte Chemie, 2021, 133, 3084-3091.	1.6	4
188	Investigation into surface composition of nitrogen-doped niobium for superconducting RF cavities. Nanotechnology, 2021, 32, 245701.	1.3	4
189	Rapid semi-quantitative analysis of hemolytic triterpenoid saponins in Lonicerae Flos crude drugs and preparations by paper spray mass spectrometry. Talanta, 2022, 239, 123148.	2.9	4
190	Parametric design approach on high-order and multi-segment modified elliptical helical gears based on virtual gear shaping. Proceedings of the Institution of Mechanical Engineers, Part C: Journal of Mechanical Engineering Science, 2022, 236, 4599-4609.	1.1	4
191	A solvent decomposition and explosion approach for boron nanoplate synthesis. Chemical Communications, 2021, 57, 4922-4925.	2.2	3
192	A Special Issue on Advanced Hybrid Nanomaterials for Energy Conversion and Storage. Science of Advanced Materials, 2019, 11, 307-310.	0.1	3
193	Optimal control of stepper motor stability program. , 2010, , .		2
194	The effects of functional polysiloxane resins on the color gamut and color yield of dyed polyester. Color Research and Application, 2012, 37, 72-75.	0.8	2
195	Analysis of Cigarette Smoke by Headspace Solid Phase Microextraction Gas Chromatography–Mass Spectrometry. Analytical Letters, 2014, 47, 1995-2002.	1.0	2
196	Water Splitting: Au Nanoparticle-Modified MoS2Nanosheet-Based Photoelectrochemical Cells for Water Splitting (Small 17/2014). Small, 2014, 10, 3536-3536.	5.2	2
197	GC–MS Investigation of the Transfer Behavior of Alkalescent Flavors in Moderate/Low-Tar Cigarettes. Chromatographia, 2014, 77, 171-178.	0.7	1
198	CdS: Phosphineâ€Free, Lowâ€Temperature Synthesis of Tetrapodâ€Shaped CdS and Its Hybrid with Au Nanoparticles (Small 22/2014). Small, 2014, 10, 4726-4726.	5.2	1

#	Article	IF	CITATIONS
199	Sensors: DNA-Templated Silver Nanoclusters for Multiplexed Fluorescent DNA Detection (Small) Tj ETQq1 1 0.784	314 rgBT	/Qverlock 10
200	Rapid microwaveâ€essisted Porter method for determination of proanthocyanidins. Phytochemical Analysis, 2020, 31, 215-220.	1.2	1
201	The anatomical, electrophysiological and histological observations of muscle contraction units in rabbits: a new perspective on nerve injury and regeneration. Neural Regeneration Research, 2022, 17, 228.	1.6	1
202	Carbon: Carbonâ€Based Sorbents with Threeâ€Đimensional Architectures for Water Remediation (Small) Tj ETQq0	0 0 0 rgBT 5.2	Overlock 1
203	Redistribution of fluorescent molecules at the solid/liquid interface with total internal reflection	2 0	0

203	illumination. Talanta, 2016, 155, 229-234.	2.9	0
204	Rücktitelbild: Liquid Nanoparticles: Manipulating the Nucleation and Growth of Nanoscale Droplets (Angew. Chem. 6/2021). Angewandte Chemie, 2021, 133, 3352-3352.	1.6	0
205	Defect-Rich, Candied Haws-Shaped AuPtNi Alloy Nanostructures for Highly Efficient Electrocatalysis. CCS Chemistry, 0, , 24-30.	4.6	0
206	Analysis of the Longitudinal-Bending-Torsional Coupled Vibration Mechanism of the Drilling of a Roof Bolter for Mine Support System. Mathematical Problems in Engineering, 2022, 2022, 1-14.	0.6	0